Available online at www.sciencedirect.com
ScienceDirect
Polymer 48 (2007) 2503–2507
polymer
www.elsevier.com/locate/polymer

Rod-like crystal growth of dioctyl substituted polyfluorene from nematic and isotropic states

Jian-Jun Zhou [a], Jing Li [a], Ya-Qin Fu [a], Zhi-Shan Bo [a,*], Lin Li [a,*], Chi-Ming Chan [b]

[a] State Key Laboratory of Polymer Physics and Chemistry, Institute of Chemistry, Chinese Academy of Sciences, Beijing 100080, China
[b] Department of Chemical Engineering, Hong Kong University of Science and Technology, Clear Water Bay, Hong Kong

Received 16 July 2006; received in revised form 5 January 2007; accepted 14 February 2007
Available online 16 February 2007

Dedicated to the memory of Professor Baotong Huang on the first anniversary of his death.

Abstract

The growth behavior of the rod-like α-form crystals from both the liquid crystal and the isotropic melt state was studied *in situ* and in real time using a hot-stage atomic force microscopy. The growth rate and direction of the poly(9,9-dioctylfluorene) (PFO) α-form crystals are greatly affected by the orientation of the polymer chains in the liquid crystal matrix. The pre-existence of chain alignment in the liquid crystal matrix serves as a precursor for crystallization, which greatly reduces the growth energy barrier and promotes the overall growth rate of PFO α-form crystals. Our results provide some valuable information for understanding the relationship between morphology and photoexcited emission behaviors.
© 2007 Elsevier Ltd. All rights reserved.

Keywords: Crystallization; Atomic force microscopy; Kinetics

1. Introduction

Polyfluorenes (PFs), which are very soluble in many solvents and produce high solid-state quantum yields, have been hailed as promising blue light-emitting materials [1–5]. However, the color instability, which is caused by a low-energy green emission band generated during operation or annealing in air, limits their practical applications [2]. The low-energy green emission has been attributed to two factors: the aggregation or the excimer formation in bulky materials [1a,3] and fluorenone defects [2]. Very recently, it has been demonstrated that the green emission band is not only related to fluorenone defects, but also to the microscopic morphology of the films [4]. Therefore, the control of the packing of the polymer chains in films is very important in the PF-based film devices to achieve improved performance. PFs, with their rigid backbone and flexible side chains, are one kind of main-chain liquid crystalline polymer. Poly(9,9-dioctylfluorene) (PFO), for example, has several types of mesophases and shows a very unique phase behavior [2,5]. It has been reported that the crystallizable semi-crystalline PFO melts near 160 °C, and then a nematic phase, which exists up to about 300 °C, occurs. Many studies were performed on the crystallization of main-chain liquid crystalline polymers from their isotropic melts, but much less information has been obtained on the role of the liquid crystal phase during crystallization. Few studies showed that the pre-existing liquid crystal phase can greatly increase the crystallization rate [6]. It has been proposed that the liquid crystal phase can serve as a precursor for crystallization, which greatly reduces the growth energy barrier. The increase of the overall crystallization rate is caused by the increase in the primary nucleation rate and the linear crystal growth rate due to the pre-existence of the liquid crystal phase. However, the morphological changes from the liquid crystal phase to the crystalline state have not been studied. We used atomic force microscopy (AFM), which has been recognized as a useful tool for the characterization of crystal growth of semi-crystalline polymers [7] in this study. The growth behavior of

* Corresponding authors. Tel./fax: +86 10 82619830.
E-mail address: lilin@iccas.ac.cn (L. Li).

0032-3861/$ - see front matter © 2007 Elsevier Ltd. All rights reserved.
doi:10.1016/j.polymer.2007.02.033

the rod-like α-form crystals from both the liquid crystal state and the isotropic melt was studied *in situ* and in real time using a hot-stage AFM. Our results provide some valuable information for understanding the relationship between morphology and photoexcited emission behaviors.

2. Experimental section

A mixture of 2,7-dibromo-9,9-dioctylfluorene and 2,7-bis(l,3,2-dioxaborinan-2-yl)-9,9-dioctylfluorene, $NaHCO_3$, tetrahydrofuran (THF) and H_2O was degassed and $Pd(PPh_3)_4$ was added to a flask under a nitrogen atmosphere. The reaction mixture was heated under reflux and stirred under nitrogen for 3 days. CH_2Cl_2 (200 mL) was added to dissolve the precipitate. The synthesis is described in Scheme 1. The organic layer was washed with water three times and dried over Na_2SO_4. After the removal of most of the solvent, the residue was precipitated in methanol. The crude polymer was purified by precipitation from THF into methanol again and dried under vacuum.

The weight-average molecular mass and polydispersity index were determined to be 5.0×10^4 and 1.6, respectively, by gel permeation chromatography using polystyrene standards. The PFO sample was dissolved in xylene with a concentration of 10 mg mL^{-1} and the solution was spin-coated onto a newly cleaved mica surface to produce a film with a thickness of about 100 nm. To prepare a frozen isotropic film, the sample was heated to 310 °C, held for 10 min and then quenched with liquid nitrogen. To prepare a frozen liquid crystal state film, the sample was heated to 220 °C, held for 10 min and then quenched with liquid nitrogen.

X-ray diffraction (XRD) profiles were obtained with a Rigaku D/max-rB X-ray diffractometer (with Ni-filtered Cu Kα radiation, $\lambda = 0.1542$ nm) operated at 40 kV and 60 mA. The scanning range varied from 3° to 30° in scanning steps of 0.02°.

AFM studies were performed using an AFM (NanoScope IIIA *MultiMode*™ Digital Instrument) equipped with a high temperature heater accessory. The temperature of the AFM hot-stage was calibrated using a thermocouple held to the mica surface by a magnetic sheet. The experimental details of the high temperature AFM are given elsewhere [7]. Si tips (TESP, Digital Instruments) with a resonance frequency of approximately 300 kHz and a spring constant of about 40 N m^{-1} were used. Both topographic and phase images were recorded simultaneously but only phase images are presented here. The hot-stage of the AFM was preset at 130 °C and the sample was placed in the AFM chamber, which was purged with argon for the protection of the sample from oxidation.

Differential scanning calorimetric (DSC) measurements were performed with a TA2910 DSC. Indium and tin were used in the temperature calibration. Samples of about 5.0 mg were sealed in aluminum pans and a nitrogen gas purge with a flux of ca. 30 mL min^{-1} was used. The heating and cooling rates were 10 °C min^{-1}.

3. Results and discussion

PFO can form various aggregates or crystal forms under different thermal treatments. The α-form crystal is the most stable one, which can be obtained at relatively low undercoolings from both the nematic and isotropic states [5d]. Fig. 1 shows XRD profiles of PFO films crystallized at 130 °C, confirming the presence of the α-form crystal [5d]. The α-form crystals are the dominant crystal structure at crystallization temperatures higher than 130 °C. The crystallization behavior of the α-form crystals provides us an ideal setting to the study of the growth behaviors of the α-form crystal from both the nematic and isotropic states *in situ* and in real time using hot-stage AFM. Rod-like α-form crystals, which randomly grew in the matrix when the film was annealed at 142 °C, are clearly seen in Fig. 2a and b. The liquid crystal matrix and the chain orientations of PFO crystals can be easily identified. In the corresponding electron diffraction, inset of Fig. 2a and b, shows two sharp reflections. These two reflections can be accounted for by the orthorhombic unit cell with parameters of $a = 2.56$ nm, $b = 2.34$ nm and $c = 3.32$ nm as (008) diffractions. This indicates that the crystals are oriented with the molecular chains in the film plane and along the normal direction of the observed rod-like structures. Moreover, even in a small area, Crystals 1, 2 and 3 grew in different directions, following the chain orientations of the matrix (cf. Fig. 2b). These results reveal that the chain orientation of the matrix has significant

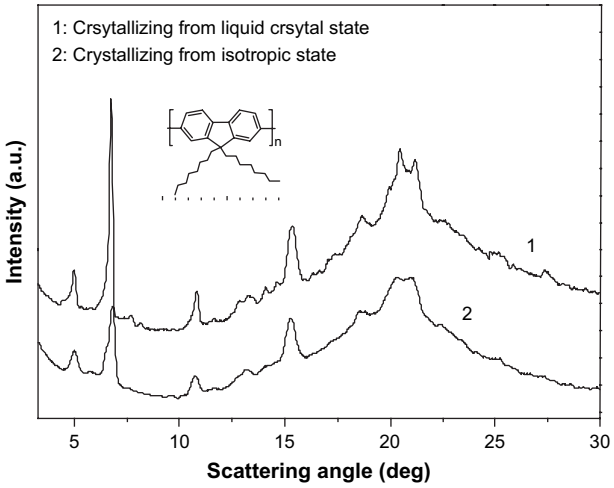

Fig. 1. XRD patterns of PFO films that crystallized at 130 °C from both the nematic (curve 1) and isotropic (curve 2) states.

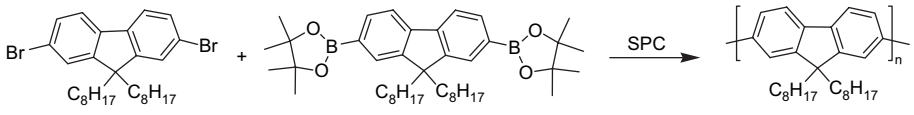

Scheme 1.

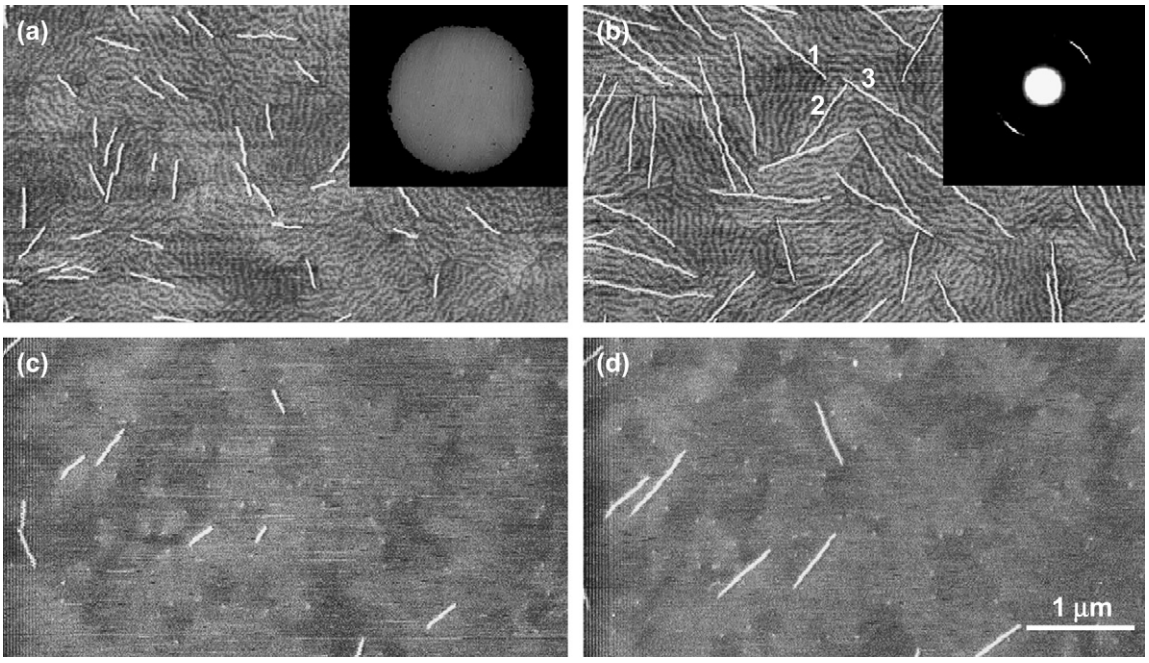

Fig. 2. *In situ* AFM observations of crystallization at 142 °C: (a) and (b) from the liquid crystal matrix with a time interval of 50 min; (c) and (d) from the isotropic matrix with a time interval of 50 min.

influence on the growth directions of the rod-like crystals. Similar rod-like crystals can be observed in the isotropic matrix at the annealing temperature of 142 °C, as shown in Fig. 2c and d. Our XRD results indicated that only the α-form crystals were obtained at relatively high undercoolings from both the nematic and isotropic states (cf. Fig. 1). Therefore, the morphologies of the crystals developed from both the nematic and isotropic states are similar to each other. However, the growth rate of the rod-like crystals in the isotropic matrix is much slower than that in the liquid matrix. The influence of the chain orientation on the growth rate and direction can be observed more clearly when the polymer crystallizes at high undercoolings. A series of AFM phase images showing the growth of rod-like crystals from the liquid crystal matrix at 132 °C are presented in Fig. 3. It is interesting to compare the growth behavior of Crystals 1 and 2. Crystal 1 grew in the same direction as the chain orientation of the matrix. Crystal 2 first grew following the chain orientation of the matrix and reached a location where the chain orientation changed, as shown in Fig. 3a and b. During the time interval

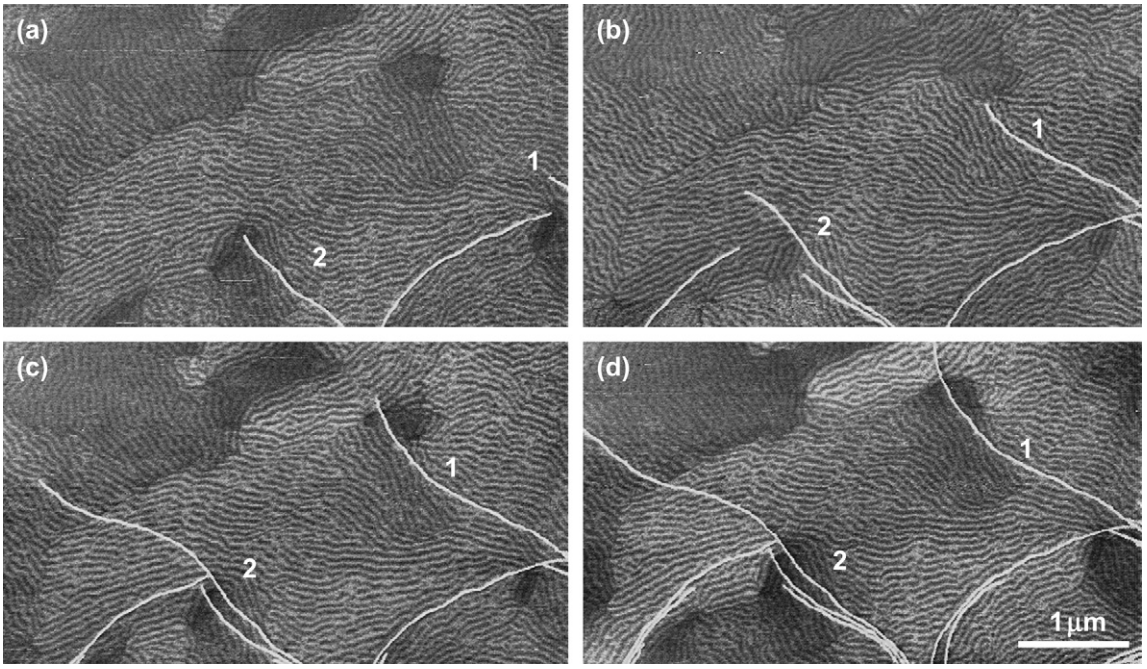

Fig. 3. *In situ* AFM observations of crystallization at 132 °C from the liquid crystal matrix, the time interval between two consecutive images was 30 min.

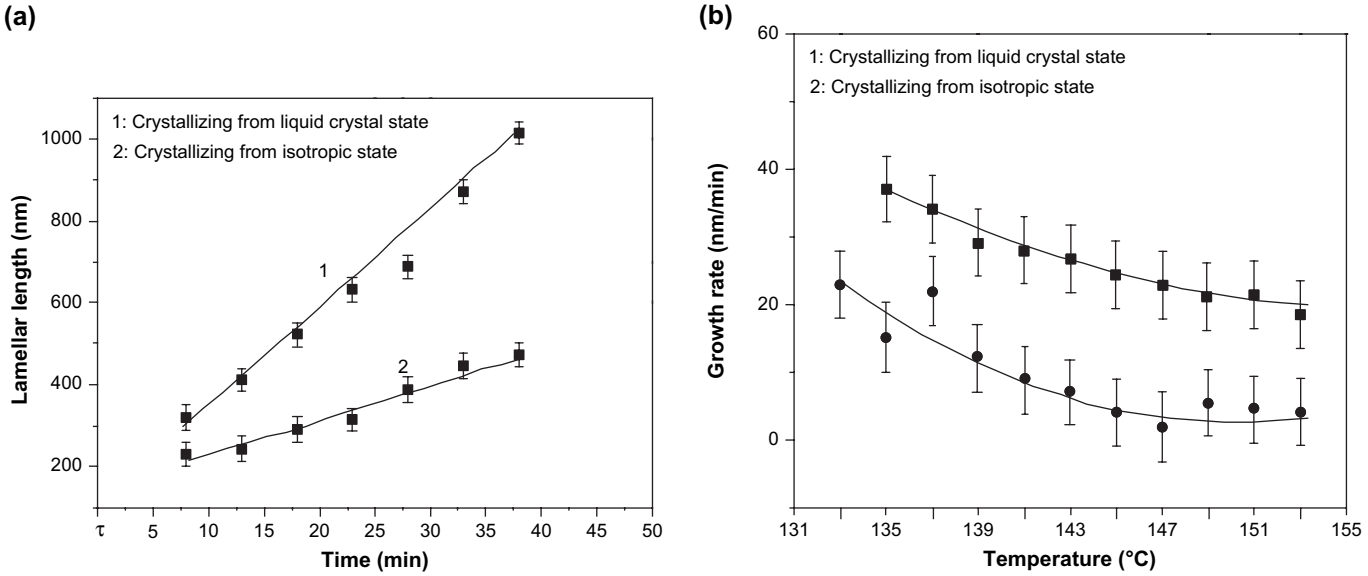

Fig. 4. (a) Lamellar length as a function of crystallization time and (b) growth rate G as a function of crystallization temperature.

between Fig. 3a and b, the lengths of Crystals 1 and 2 were found to increase about 1.3 and 0.7 μm, respectively, showing that the growth rate of rod-like crystals decreases when the chain orientation of the matrix changes. After passing the region where the change in the chain orientation occurred, Crystal 2 bended left and its growth rate increased and its growth direction again followed the chain orientation of the matrix, as shown in Fig. 3c and d. When Crystal 1 reached a location where there was a change in the chain orientation of the matrix, a similar phenomenon was observed (cf. Fig. 3b and c). Our results clearly show that the orientation of polymer chains in liquid crystal matrix can influence both the growth rate and growth direction of rod-like crystals.

The length of rod-like crystal along its growth direction versus time at 140 °C was measured using AFM. The results are shown in Fig. 4a. Although the growth rate of

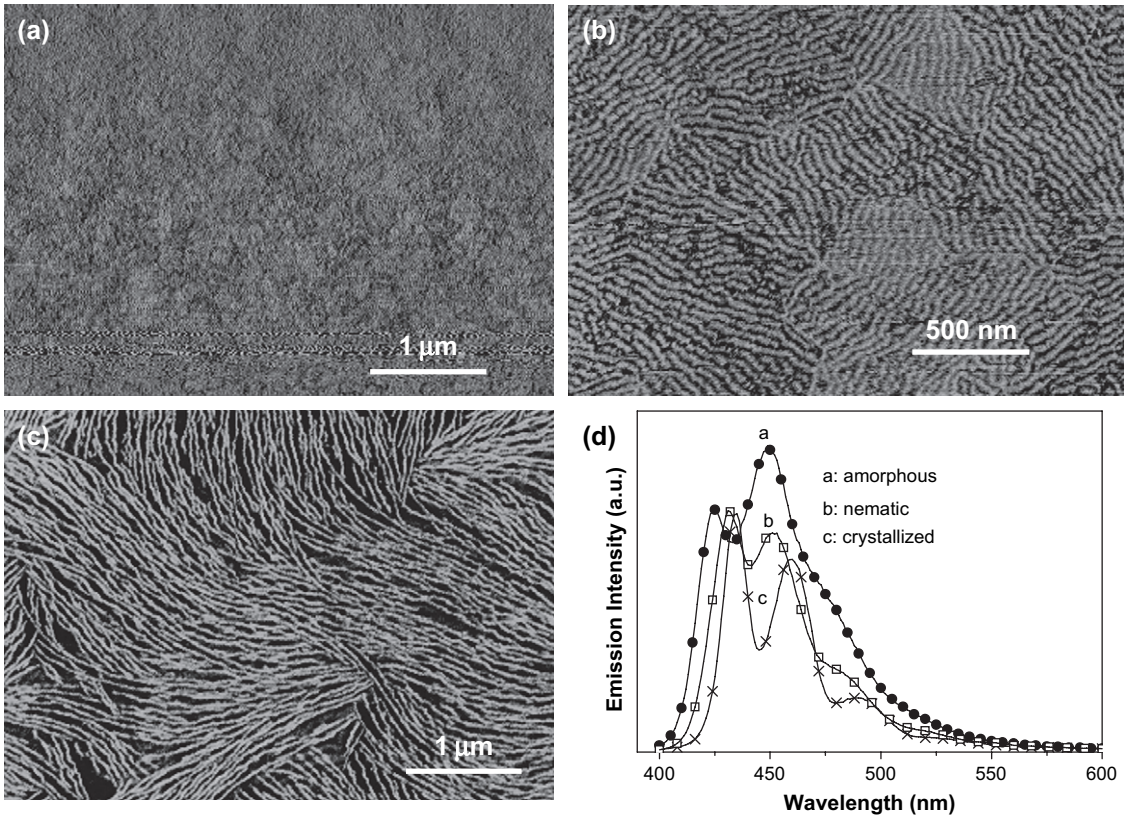

Fig. 5. Morphologies and the emission spectra of: (a) amorphous, (b) liquid crystal and (c) α-form crystal films.

the crystals decreases when the chain orientation changes, the average growth rate stays relatively constant, as shown in Fig. 4a. Plots showing the average growth rate of the rod-like crystals in both the liquid crystal and isotropic states at different temperatures are presented in Fig. 4b. The average growth rate in the liquid crystal matrix is about twice that in the isotropic state. Therefore, the pre-existence of the polymer chain orientation greatly increases the growth rate of the α-form crystals. In addition, a careful examination of Fig. 2 indicates that within a fixed period of time, the number of rod-like crystals formed on a liquid crystal matrix was much larger than that formed on an isotropic matrix. These results suggest that the chain orientation in the liquid crystal matrix can significantly increase the primary nucleating rate and the linear growth rate of the α-form crystals. Consequently, the growth of the rod-like crystals is much easier in the nematic state than that in the isotropic state. In order to understand the contributions of aggregation and crystallization effects on the green band emission of PFO films, the photoluminescence spectra are shown in Fig. 5. The emission spectra clearly show a red-shift for the PFO films in the amorphous state, liquid crystal phase and α-form crystal phase. However, the green emission band cannot be observed in the spectra.

In summary, we conclude that the primary nucleation rate and the lamellar growth rate as well as direction of the PFO α-form crystals are greatly affected by the orientation of the polymer chains in the liquid crystal matrix. The pre-existence of chain alignment in the liquid crystal matrix serves as a precursor for crystallization, which greatly reduces the primary nucleation barrier and the growth energy barrier, leading to an increased primary nucleating rate and increased linear growth rate of PFO α-form crystals. The color stability will be improved if PFO films are annealed to develop more stable α-form crystals from the nematic phase. Our results may provide important guidance in developing many practical applications using fluorene-based polymers.

Acknowledgments

We are grateful for the support of the Outstanding Youth Fund and National Science Foundation of China (Grant Nos. 20325414, 20574083, 50521302, 20634050).

References

[1] (a) Grell M, Bradley DC, Ungar G, Hill J, Whitehead KS. Macromolecules 1999;32:5810–7;
(b) Herz LM, Phillips RT. Phys Rev B 2000;61:13691–7;
(c) Teetsov J, Vanden Bout DA. J Am Chem Soc 2001;123:3605–6;
(d) Winokur MJ, Slinker J, Huber DL. Phys Rev B 2003;67:184106–17.
[2] Scherf U, List EWJ. Adv Mater 2002;14:477–87.
[3] Neher D. Macromol Rapid Commun 2001;22:1365–85.
[4] Surin M, Hennebicq E, Ego C, Marsitzky D, Grimsdale AC, Müllen K, et al. Chem Mater 2004;16:994–1001.
[5] (a) Teesov J, Fox MA. J Mater Chem 1999;9:2117–22;
(b) Blondin P, Bouchard J, Beaupre S, Belletete M, Durocher G, Leclerc M. Macromolecules 2000;33:5874–9;
(c) Kawana S, Durrell M, Lu J, Macdonald JE, Grell M, Bradley DDC, et al. Polymer 2002;43:1907–13;
(d) Chen SH, Su AC, Su CH, Chen SA. Macromolecules 2005;38:379–85.
[6] (a) Yandrasits MA, Cheng SZD, Zhang AQ, Cheng JL, Wunderlich B, Percec V. Macromolecules 1992;25:2112–21;
(b) Pardey R, Zhang AQ, Gabori PA, Harris FW, Cheng SZD, Adduci J, et al. Macromolecules 1992;25:5060–8;
(c) Pardey R, Shen DX, Gabori PA, Harris FW, Cheng SZD, Adduci J, et al. Macromolecules 1993;26:3687–97;
(d) Pardey R, Wu SS, Chen JH, Harris FW, Cheng SZD, Keller A, et al. Macromolecules 1994;27:5794–802;
(e) Jing AJ, Taikum O, Li CY, Harris FW, Cheng SZD. Polymer 2002;43:3431–40.
[7] (a) Pear R, Vancso GJ. Macromolecules 1997;30:5843–8;
(b) Godovsky YK, Magonov SN. Langmuir 2000;16:3549–52;
(c) Hobbs JK, Humphris ADL, Miles MJ. Macromolecules 2001;34:5508–19;
(d) Li L, Chan CM, Yeung KL, Li JX, Ng KM, Lei YG. Macromolecules 2001;34:316–25;
(e) Lei YG, Chan CM, Li JX, Ng KM, Wang Y, Jiang Y, et al. Macromolecules 2002;35:6751–3;
(f) Jiang Y, Yan DD, Gao X, Han CC, Jin XG, Li L, et al. Macromolecules 2003;36:3652–5;
(g) Xu J, Guo BH, Zhang ZM, Zhou JJ, Jiang Y, Yan S, et al. Macromolecules 2004;37:4118–23.